

GETTING TO KNOW OUR SPACE POPULATION FROM THE PUBLIC CATALOG

Daniel L. Oltrogge* and T.S. Kelso*

Our space population continues to increase as satellites are launched and debris-producing catastrophic events occur. For operators and policy makers, a periodic examination of the publicly available space population is useful. In this paper, bivariate distributions and visualizations of orbital elements and simple spatial density metrics clearly delineate regions of higher collision risk. For the highest risk region, benefits obtained by application of ISO orbital debris mitigation standards are discussed. Application of concentric spherical zone "Ring Shells" governed in latitude by object maximum latitude distribution helps provide a more realistic spatial density and collision probability picture compared with previous analyses.

INTRODUCTION

The space population continues to increase at an unsteady rate, averaging roughly 300 new Resident Space Objects (RSOs) per year according to publicly-available, historical Non-Cooperative Tracking (NCT) data. As shown in Figure 1, this RSO increase has experienced

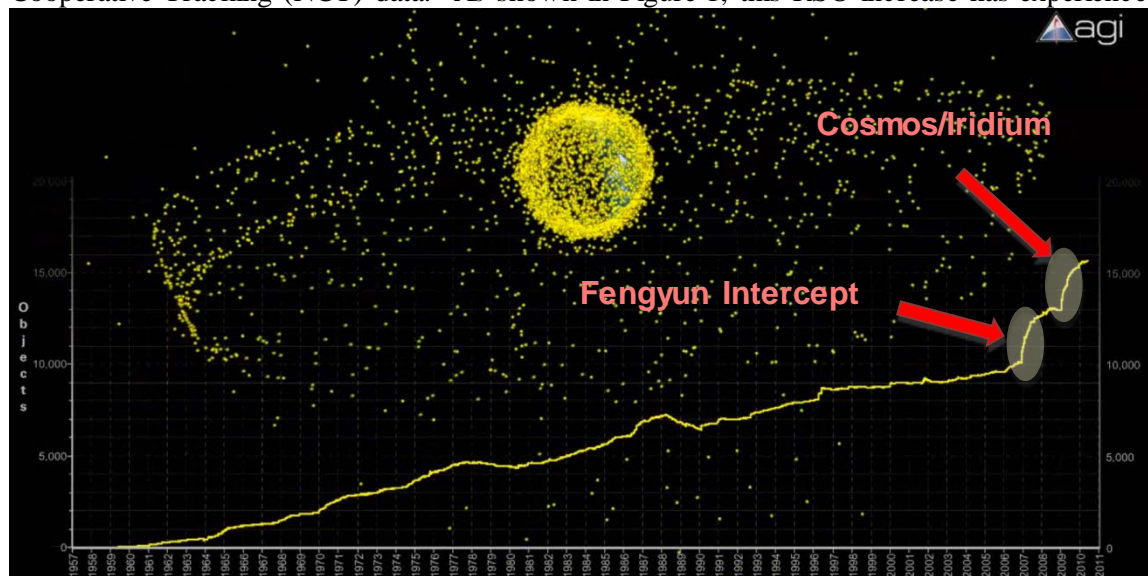


Figure 1. Evolution of the Resident Space Population from 1957 to Present

* Senior Research Astrodynamist, AGI's Center for Space Standards and Innovation, 7150 Campus Drive, Suite 260, Colorado Springs, CO 80920.

growth spurts due to catastrophic debris-creating events such as the Iridium/Cosmos collision in 2007 and the Fengyun ASAT intercept in 2008.

This fresh examination of the space population was undertaken on behalf of the Space Data Association Ltd. (SDA), a non-profit organization that brings together satellite operators who value the controlled, reliable and efficient data-sharing that is critical to the safety and integrity of the space environment and the Radio Frequency (RF) spectrum. The SDA was founded by Inmarsat, Intelsat and SES — three of the leading global satellite communications companies. By collecting and analyzing definitive SDA Member RF, Conjunction Assessment (CA), ephemeris data, the SDA's Space Data Center (SDC) is able to perform Space Situational Awareness and threat mitigation analyses with previously unachievable accuracy. Currently, the SDA membership spans both GEO and LEO regimes, with over sixty percent of GEO satellites operated by SDA members.

DATA SOURCES

The space population was characterized using on-orbit (i.e., non-decayed) RSOs, based upon the 22 February 2011 Satellite Catalog maintained at www.CelesTrak.com. A variety of single and bivariate distributions were then taken of the data, including:

- Perigee Versus Apogee Altitude Distribution
- Maximum Latitude Versus Altitude Distribution
- Origination Year Versus Altitude Distribution
- Spatial Density Versus Altitude Distribution
- Eccentricity Versus Altitude Distribution
- RCS Versus Altitude Distribution
- Inclination Versus Altitude Distribution
- Collision Probability Versus Perigee and Apogee Altitudes

Satellite Catalog (SATCAT)

Search Form

Data current as of 2011 July 22

Select one:

- ☒ Name
- ☐ International Designator
- ☐ NORAD Catalog Number

☒ Payloads only Maximum responses: 250

Notes:

- The Name field may use any portion of the satellite name.
- The International Designator has a format of YYYY-MMNAAA (e.g., 1994-029AAB).
- Any portion may be used (e.g., 2011-).
- The NORAD Catalog Number is a 1- to 5-digit number.

[Raw SATCAT Data](#)

[SATCAT Format Documentation](#)

	TLE Data	Space Data	
	Current	GPS	
	Archives	EOP	
	Documentation	Space Weather	
	SATCAT	Columns	
Boxscore	Software		
SOCRATES			

Figure 2. CelesTrak SATCAT download link

SPACE POPULATION DISTRIBUTION BY ALTITUDE

By accumulating the distribution in satellite perigee and apogee altitudes, the entire space population can be categorized. The resulting perigee-vs-apogee distribution for the public space population is shown in Figure 3 and Figure 4.

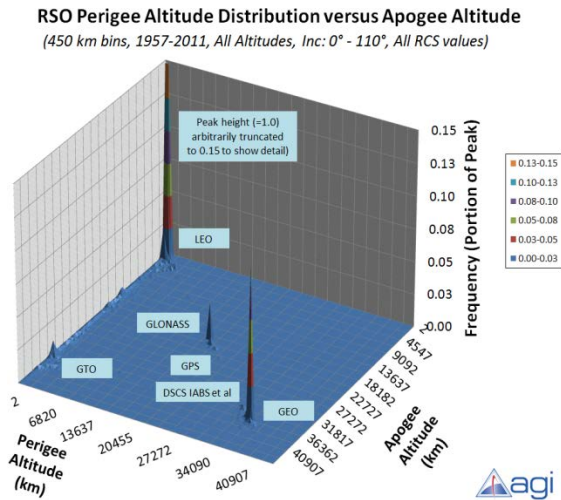


Figure 3. Space Population Perigee-vs-Apogee Distribution (3D)

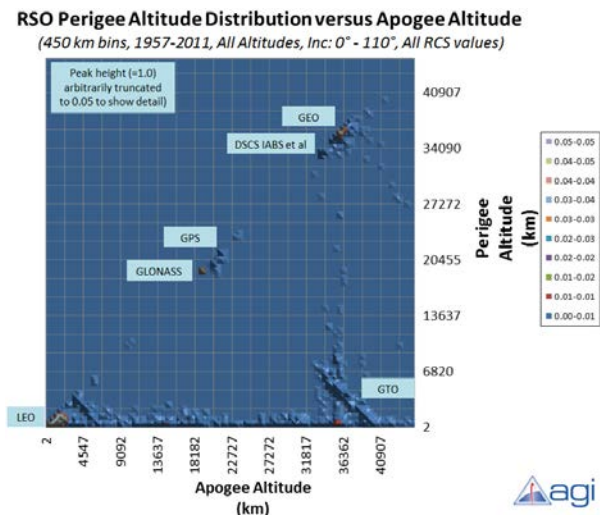


Figure 4. Space Population Perigee-vs-Apogee Distribution (2D)

Altitude Distribution Statistics

It is also of interest to examine the minimum, median and maximum perigee altitude values as a function of apogee altitude, as shown in Figure 5.

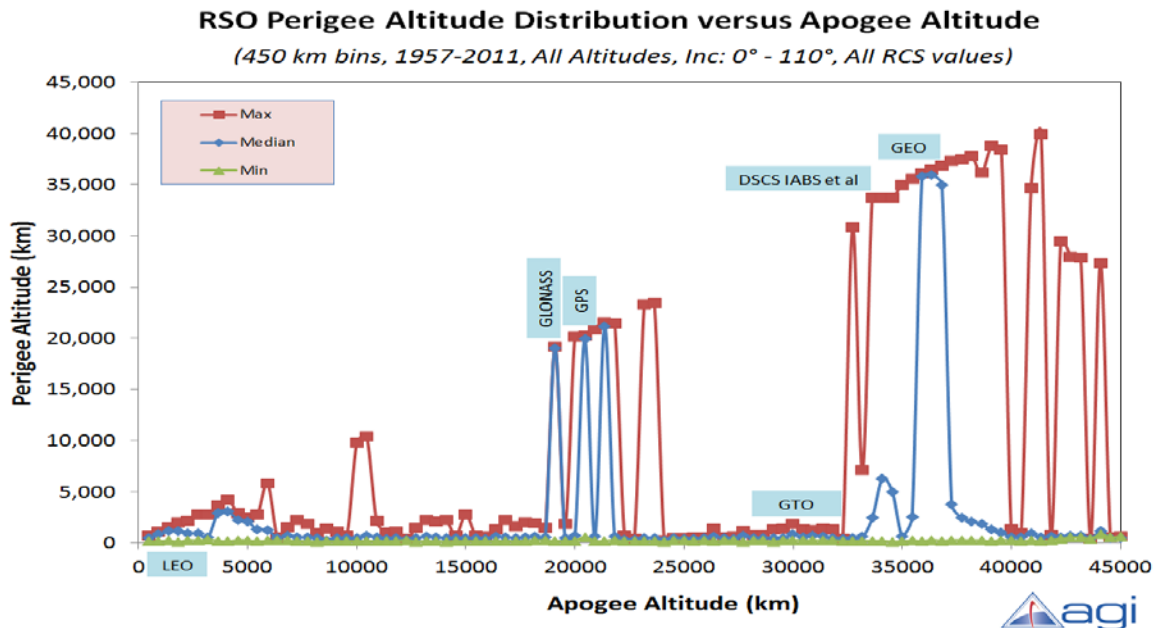


Figure 5. RSO Perigee Altitude Distribution Statistics as Function of Apogee Altitude

LEO ALTITUDE DISTRIBUTION STATISTICS

The Low-Earth Orbit (LEO) regime (altitude ranging from 0 to 2000 km) is characterized as shown in Figure 6 and Figure 7. In these views, the circular orbits (along the diagonal line, which defines a circular orbit) ranging from 450 to 1000 km are more heavily populated. Additionally, the Iridium and Fenyun 1C catastrophic debris-creating events can be clearly seen as bands of RSOs running along fixed apogee and perigee lines.

RSO Perigee Altitude Distribution versus Apogee Altitude (LEO)
(20 km bins, 1957-2011, LEO Only, All Altitudes, Inc: 0° - 110°)

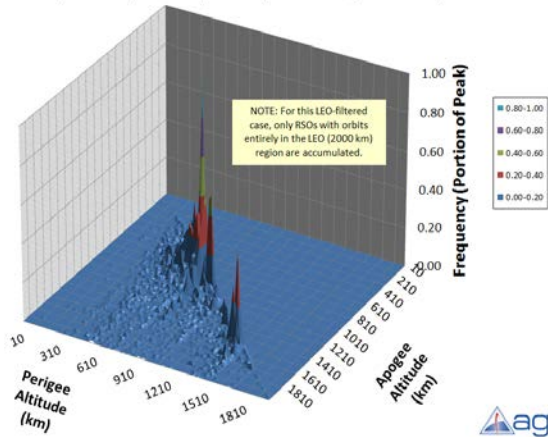


Figure 6. LEO Space Population Perigee-vs-Apogee Distribution (3D)

RSO Perigee Altitude Distribution versus Apogee Altitude (LEO)
(20 km bins, 1957-2011, LEO Only, All Altitudes, Inc: 0° - 110°)

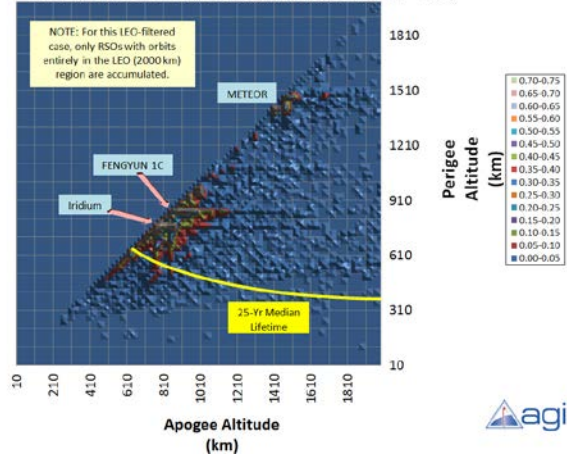


Figure 7. LEO Space Population Perigee-vs-Apogee Distribution (2D)

Figure 7 and Figure 8 show an enlarged view of the LEO regime, focusing upon the most highly populated regions. As was the case in Figure 7, the ISO Standard 25-year median orbit lifetime curve has been inserted corresponding to a ballistic coefficient¹ of $\beta = 181.6 \text{ cm}^2 / \text{kg}$. The figure shows that the preponderance of LEO RSO population will remain on orbit for a very long time.

RSO Perigee Altitude Distribution versus Apogee Altitude (LEO)
(8 km bins, 1957-2011, LEO Only, Inc: 0° - 110°, All RCS values)

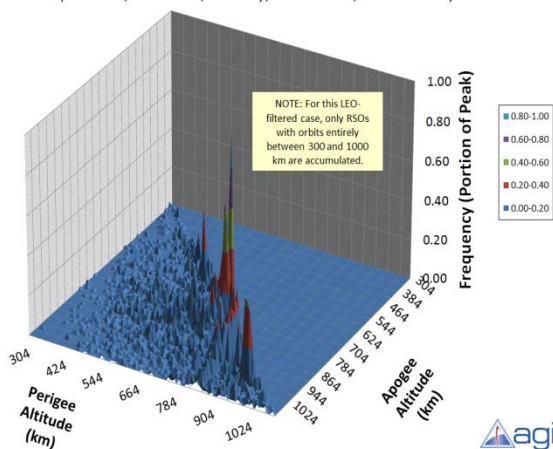


Figure 8. LEO Space Population Perigee-vs-Apogee Distribution (Zoom-in, 3D)

RSO Perigee Altitude Distribution versus Apogee Altitude (LEO)
(8 km bins, 1957-2011, LEO Only, Inc: 0° - 110°, All RCS values)

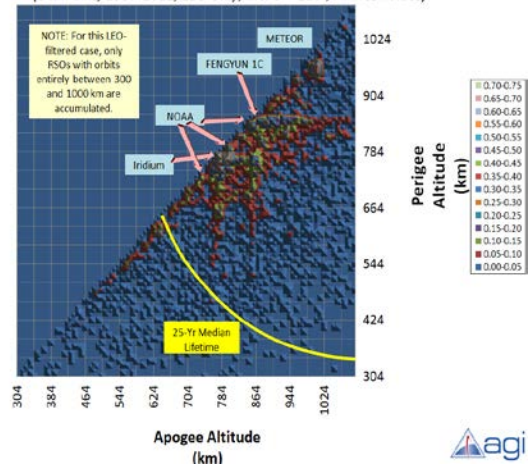


Figure 9. LEO Space Population Perigee-vs-Apogee Distribution (Zoom-in, 2D)

MEO ALTITUDE DISTRIBUTION STATISTICS

As Figure 4 showed, the Middle-Earth Orbit (MEO) regime is sparsely populated except for the GLONASS and GPS constellations. Accordingly, we focus our MEO examination on these two orbits as shown in Figure 10 and Figure 11. The GLONASS constellation is observed to be more tightly controlled in a circular orbit than the control in the GPS system.

RSO Perigee Altitude Distribution versus Apogee Altitude (MEO)
(30 km bins, 1957-2011, MEO Only, Inc: 0° - 110°, All RCS values)

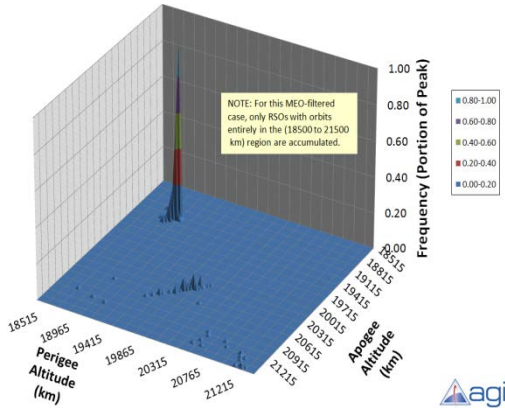


Figure 10. MEO Space Population Perigee-vs-Apogee Distribution (Zoom-in, 3D)

RSO Perigee Altitude Distribution versus Apogee Altitude (MEO)
(30 km bins, 1957-2011, MEO Only, Inc: 0° - 110°, All RCS values)

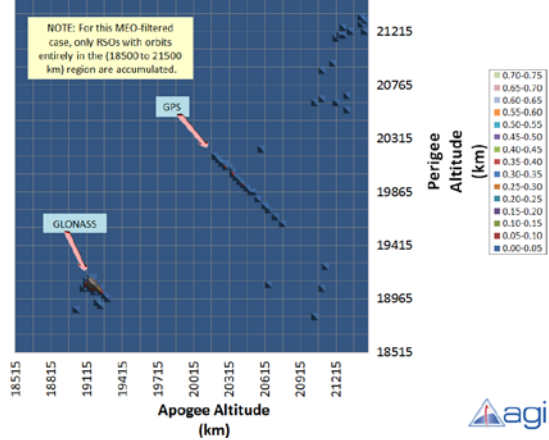


Figure 11. MEO Space Population Perigee-vs-Apogee Distribution (Zoom-in, 2D)

GEO ALTITUDE DISTRIBUTION STATISTICS

The Geosynchronous Earth Orbit (GEO) population distribution is shown in Figure 12 and Figure 13. In these plots, the large spike of GEO satellites is evident. A small spike of DSCS Integrated Apogee Boost Systems (IABS) and similar objects are seen below GEO altitude; these upper stages raised the satellite's orbit nearly to GEO and allowed the satellite to complete the ascent to its orbital station.

RSO Perigee Altitude Distribution versus Apogee Altitude (GEO)
(35 km bins, 1957-2011, GEO Only, All Altitudes, Inc: 0° - 110°)

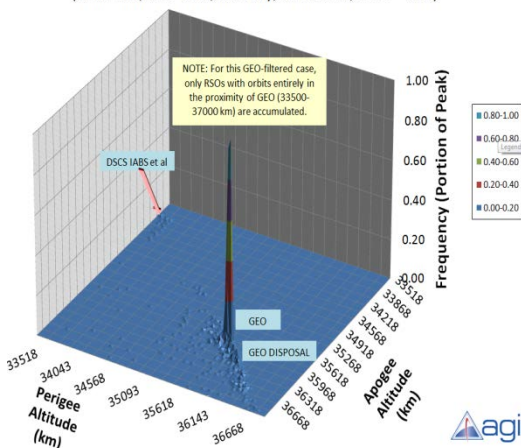


Figure 12. GEO Space Population Perigee-vs-Apogee Distribution (3D)

RSO Perigee Altitude Distribution versus Apogee Altitude (GEO)
(35 km bins, 1957-2011, GEO Only, All Altitudes, Inc: 0° - 110°)

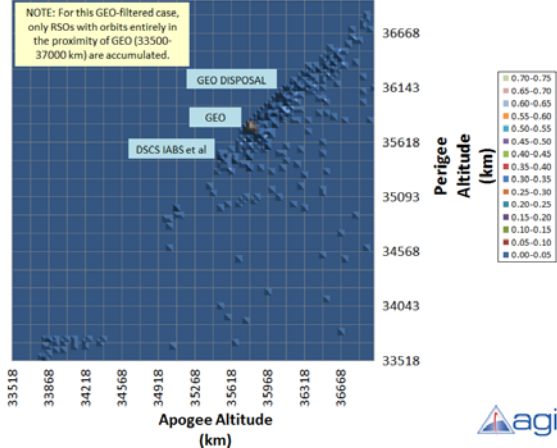


Figure 13. GEO Space Population Perigee-vs-Apogee Distribution (2D)

ORIGINATION YEAR DISTRIBUTION STATISTICS

One metric retained in the Space Object catalog is the origination year for the satellite or debris object of interest. This metric can be misleading: it is not the year that the object originated in space, but rather the year that the object was first deployed in space. Fragments that stemmed from a catastrophic debris-causing event (e.g. Fengyun-1C) are assigned the date of the Fengyun-1C deployment in space, as opposed to the actual debris-causing intercept.

It is interesting to observe the development of the various orbital regimes in Figure 14 and Figure 15. The year of occupancy for a given circular orbit can plainly be seen, in addition to the upper stages and boosters required to place the satellite in those circular orbits.

Major fragmentation events can be observed in Figure 16 and Figure 17, as attributable to Cosmos 2251 (launched in 1993) & Iridium (1997) collision and Fengyun Intercept events.

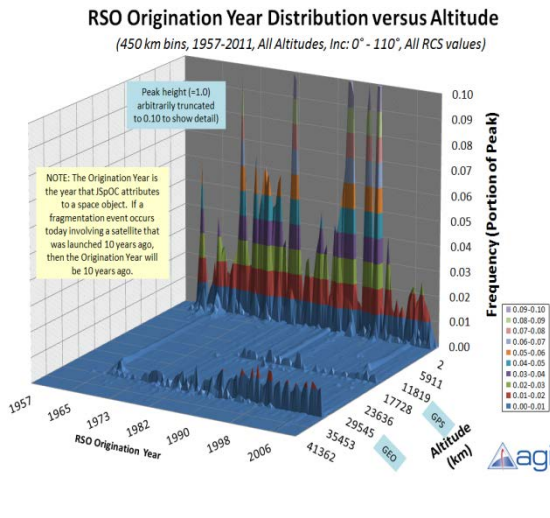


Figure 14. RSO Origination Year vs Altitude (3D)

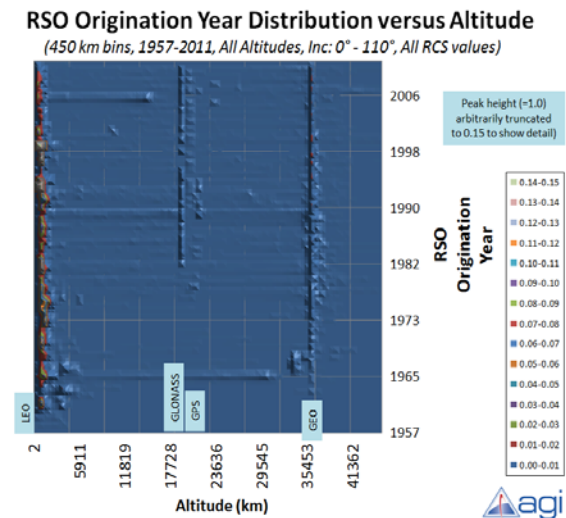


Figure 15. RSO Origination Year vs Altitude (2D)

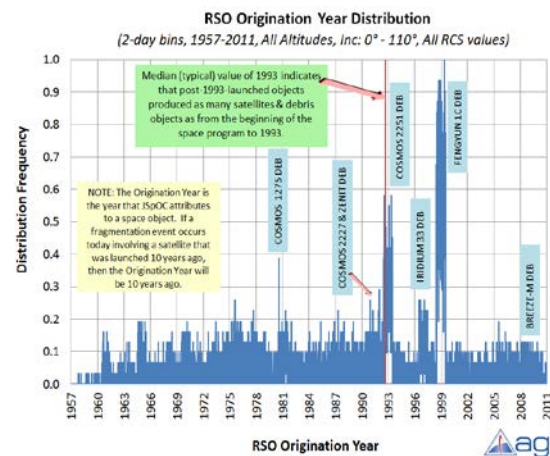


Figure 16. RSO Origination Year

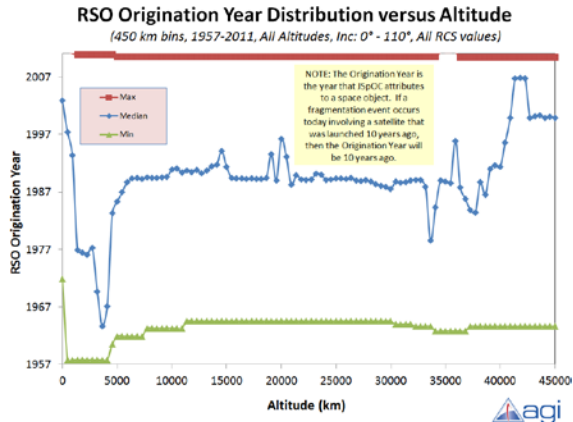


Figure 17. RSO Origination Year Distribution Statistics

CATALOG INTRODUCTION YEAR DISTRIBUTION STATISTICS

A more interesting and representative distribution is that of the Space Object catalog introduction date for each fragment. This is the year that the object was first introduced into the public space catalog. Fragments that stemmed from a catastrophic debris-causing event (e.g. Fengyun-1C) are assigned to the actual debris-causing intercept time.

The evolution of the various orbital regimes is shown in Figure 18 and Figure 19. The year of occupancy for a given circular orbit can plainly be seen, in addition to the upper stages and boosters required to place the satellite in those circular orbits. The dominant introduction of debris from major fragmentation events (2007 Fengyun-1C intercept and 2009 Cosmos 2251/Iridium 33 collision) can be observed. These debris events are also prominent features in Figure 20 and Figure 21.

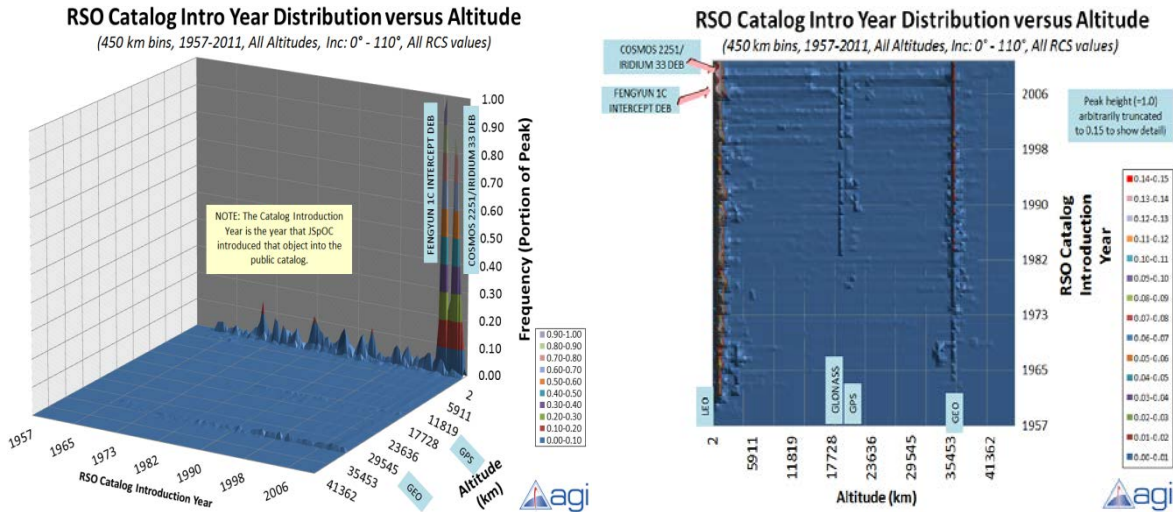


Figure 18. RSO Catalog Intro Year vs Altitude (3D)

Figure 19. RSO Catalog Intro Year vs Altitude (2D)

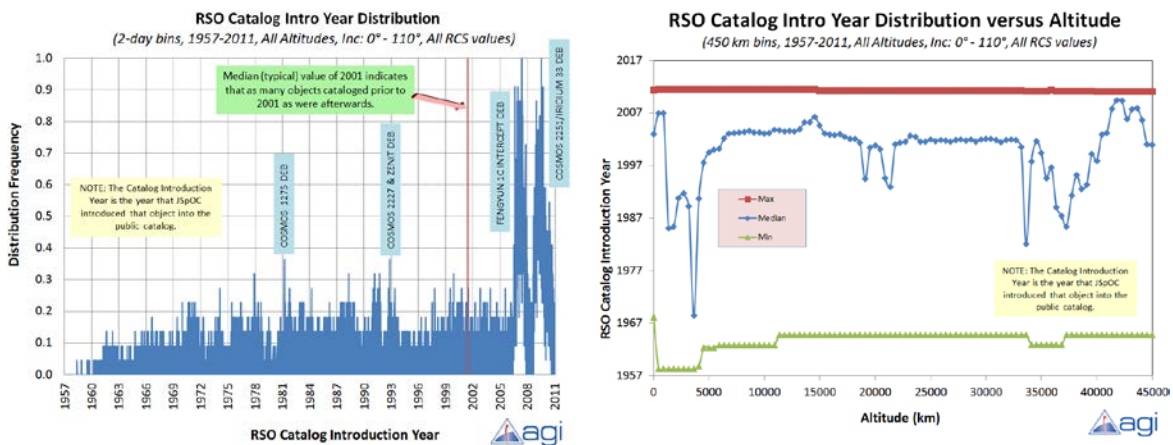


Figure 20. RSO Catalog Intro Year

Figure 21. RSO Catalog Intro Year Distribution Statistics

ECCENTRICITY DISTRIBUTION STATISTICS

Eccentricity distributions readily separate circular orbits from both transfer & operational elliptical orbits, as shown in Figure 22 and Figure 23. Overall eccentricity distribution and related statistics are shown in Figure 24 and Figure 25.

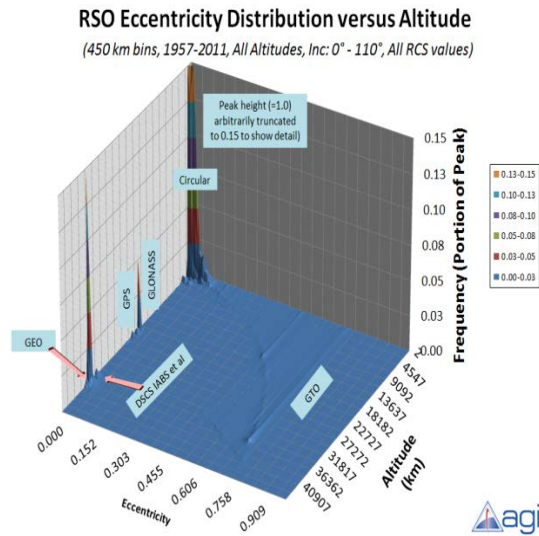


Figure 22. RSO Eccentricity Distribution (3D)

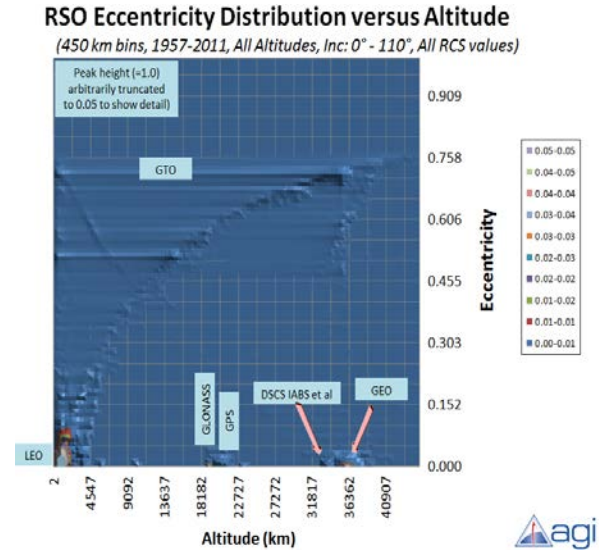


Figure 23. RSO Eccentricity Distribution (2D)

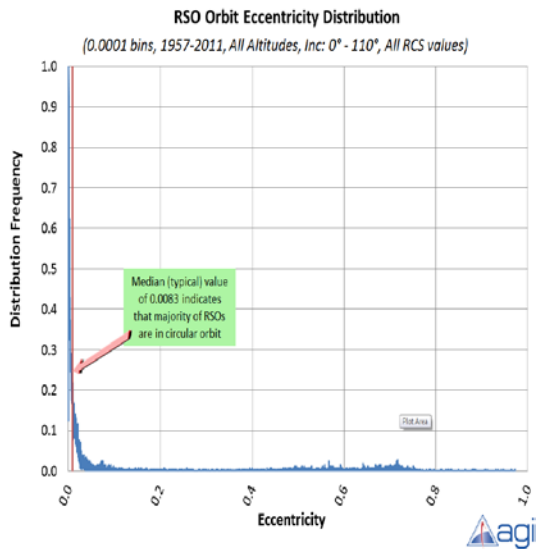


Figure 24. RSO Eccentricity Distribution

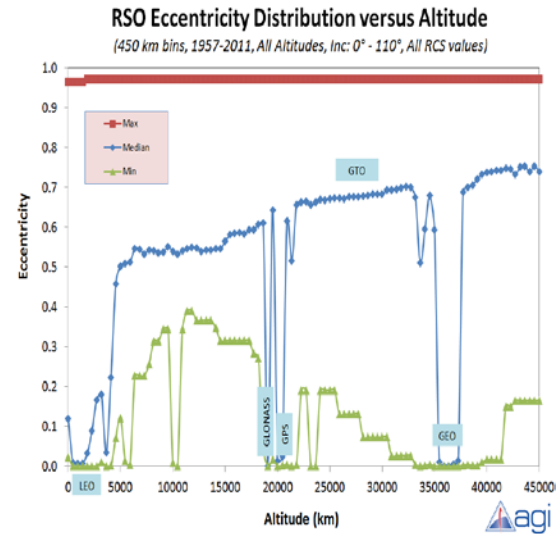


Figure 25. RSO Eccentricity Distribution Statistics

INCLINATION DISTRIBUTION STATISTICS

Inclination distributions readily differentiate between various constellations and launch site transfer orbits, as shown in Figure 26 and Figure 27. Overall eccentricity distribution and related statistics are shown in Figure 28 and Figure 29.

RSO Orbit Inclination Distribution versus Altitude

(450 km bins, 1957-2011, All Altitudes, Inc: 0° - 110°, All RCS values)

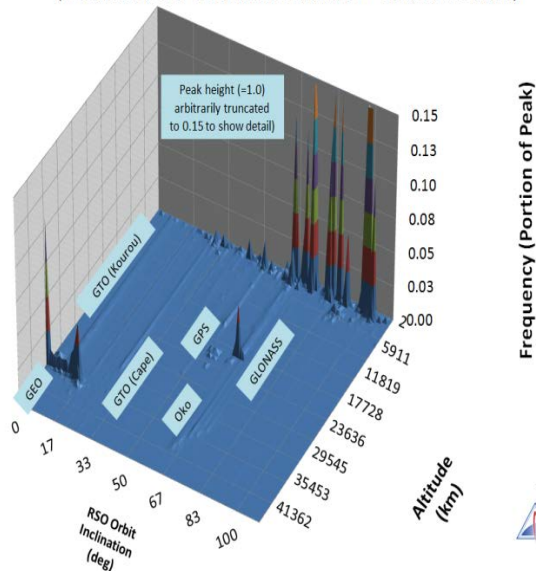


Figure 26. RSO Inclination Distribution (3D)

RSO Orbit Inclination Distribution versus Altitude

(450 km bins, 1957-2011, All Altitudes, Inc: 0° - 110°, All RCS values)

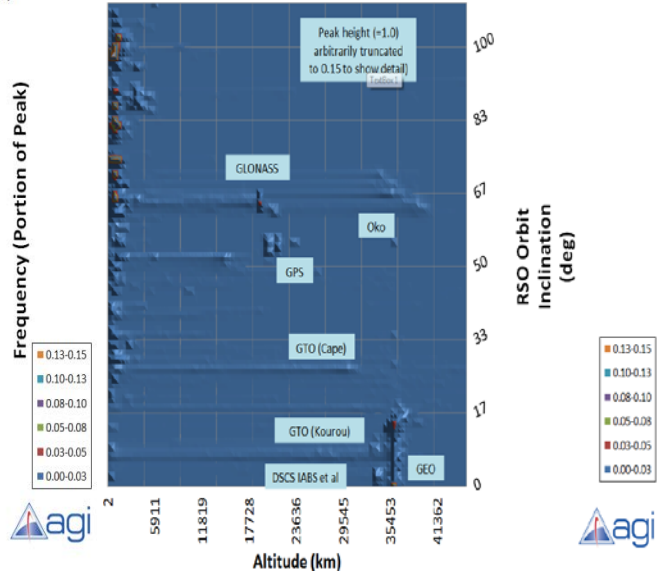


Figure 27. RSO Inclination Distribution (2D)

RSO Orbit Inclination Distribution

(0.01 deg bins, 1957-2011, All Altitudes, Inc: 0° - 110°, All RCS values)

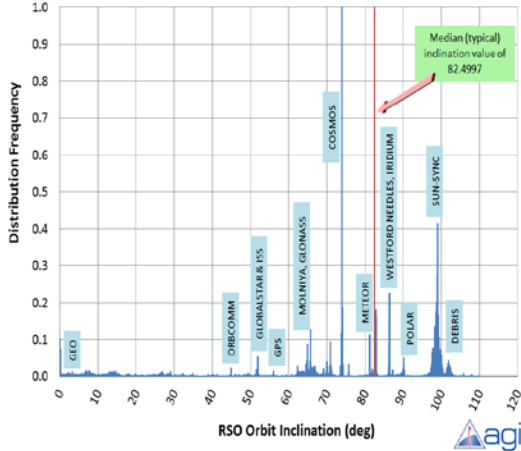


Figure 28. RSO Inclination Distribution

RSO Orbit Inclination Distribution versus Altitude

(450 km bins, 1957-2011, All Altitudes, Inc: 0° - 110°, All RCS values)

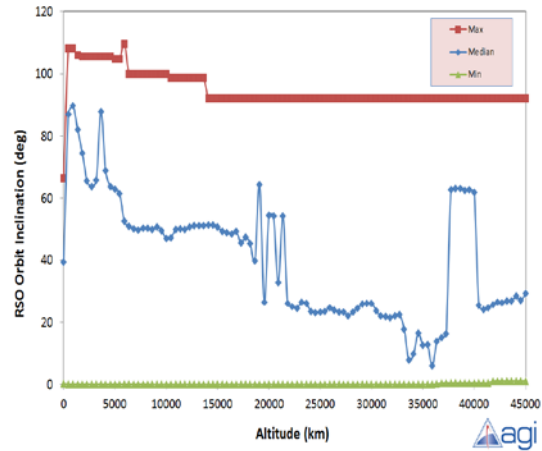


Figure 29. RSO Inclination Distribution Statistics

PERCENT OF SATELLITES THAT ARE OPERATIONAL

Using satellite operational status code from CelesTrak (Figure 32), the distribution in percent of Resident Space Objects that are operational can be determined (Figure 33). The chart is cropped at 0.15 so more detail can be shown. While debris dominates the percent of objects at LEO, while operational satellites comprise as much as thirty percent in the GEO regime.

SATCAT Operational Status

Operational Status	Descriptions
+	Operational
-	Nonoperational
P	Partially Operational
B	Backup/Standby
S	Spare
X	Extended Mission
D	Decayed
?	Unknown

RSO %Operational Distribution versus Altitude

(450 km bins, 1957-2011, All Altitudes, Inc: 0° - 110°, All RCS values)

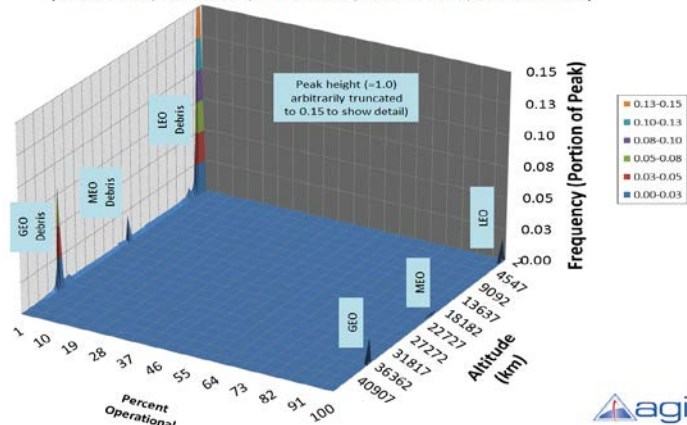


Figure 30. Operational Status Legend

Figure 31. RSO Percent Operational Distribution

MAXIMUM LATITUDE DISTRIBUTION STATISTICS

Maximum latitude distribution (Figure 30) and median value (Figure 31) provide a method to define “Ring Shells” for typical satellite spatial density calculations. We will use the median value of maximum latitude as a function of altitude in the next section.

RSO Maximum Latitude Distribution versus Altitude

(450 km bins, 1957-2011, All Altitudes, Inc: 0° - 110°, All RCS values)

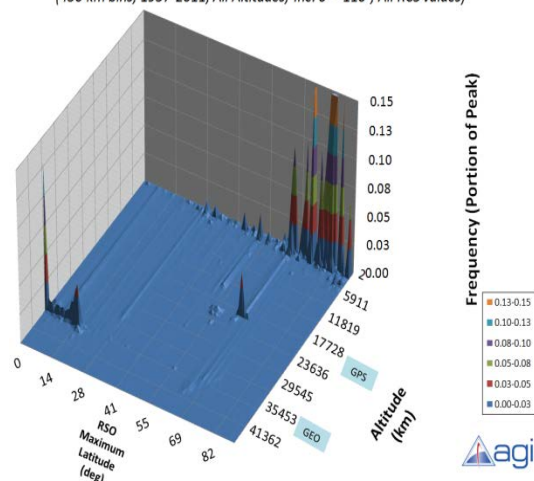


Figure 32. Maximum Latitude Distribution

RSO Maximum Latitude Distribution versus Altitude

(450 km bins, 1957-2011, All Altitudes, Inc: 0° - 110°, All RCS values)

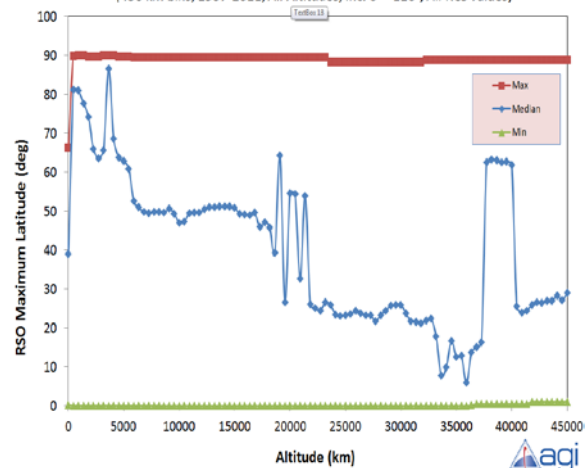


Figure 33. Maximum Latitude Distribution (1D)

SPACE POPULATION SPATIAL DENSITY DISTRIBUTION STATISTICS

Spatial density has often been used to define the number of RSOs per unit volume as a function of altitude. This computation is performed by “flying” each satellite through concentric shells, and accumulating the portion of each orbit that flies through a given shell. After the entire space population is accumulated, the analyst can simply divide the number of objects contained within a concentric shell by the volume of the shell to yield spatial density at that shell’s altitude, as shown in Figure 34.

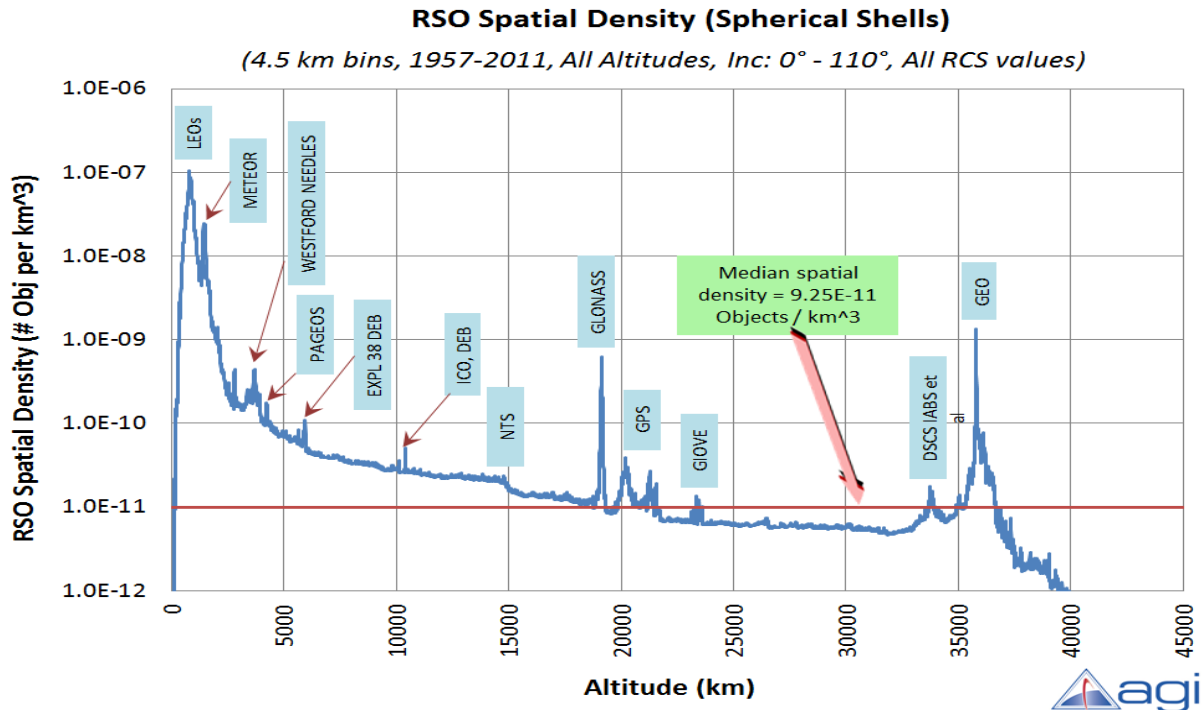


Figure 34. RSO Spatial Density Using Spherical Shells

The spatial density plot allows the user to readily identify various constituents of the space population, as the identification tabs show. The user can also see that the spatial density of the GEO population is several orders of magnitude below that of the LEO population.

However, by revisiting Figure 30 and Figure 31, we can see that the underlying assumption of spherical shells is flawed. Whereas in the LEO regime it is very common to get high orbit inclinations (yielding high maximum latitudes), it is rare to get high maximum latitudes in the GEO regime. Generalizing this observation, we see that dividing the population by a spherical shell volume is therefore misleading, because the objects don’t really occupy the entire shell.

A more realistic approach is to adopt a “Ring Shell,” defined to be a ring bounded by the upper and lower spherical zones spanning the latitude range between \pm (maximum latitude). The result is shown in Figure 35. We can now observe that spatial density is actually slightly higher in the GEO regime than it is in LEO.

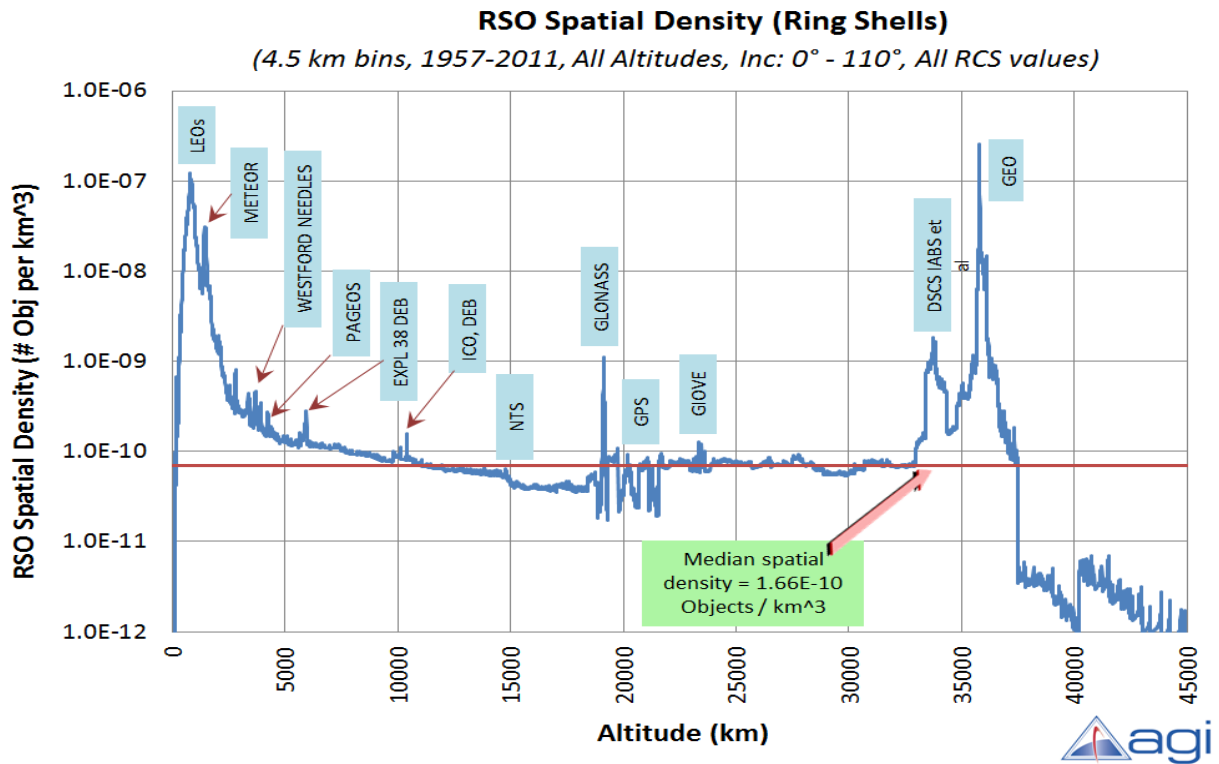


Figure 35. RSO Spatial Density Using Ring Shells

RADAR CROSS SECTION DISTRIBUTION STATISTICS

As shown in Figure 36 and Figure 37, Radar Cross Section (RCS) distribution exhibits a fairly uniform trend, with slight emphasis on tracking larger objects at GEO altitudes (as expected). Note in Figure 37 that a median RCS value has been obtained as a function of altitude; this profile will be used in the next section.

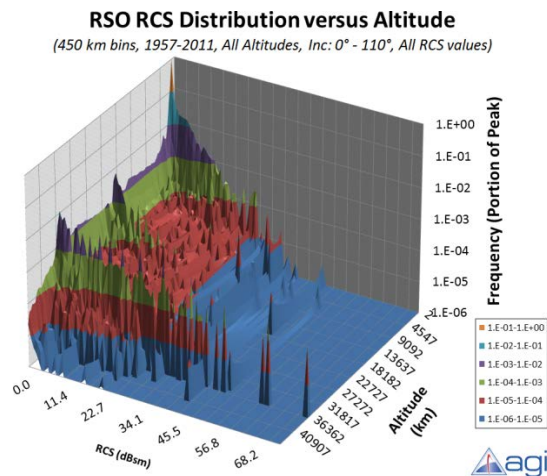


Figure 36. RSO RCS Distribution (3D)

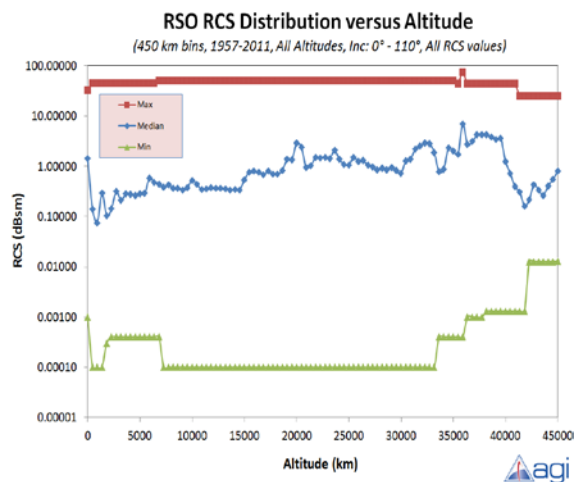


Figure 37. RSO RCS Versus Altitude

COLLISION PROBABILITY DISTRIBUTION STATISTICS

By making additional assumptions and adopting the “Ring Shell” spatial density profile, we can now determine collision probability on an annual basis. The required simplifying assumptions are that: (1) the portion of time a primary object spends flying through each “Ring Shell” is dictated only by its flight path angle and altitude; (2) objects are randomly distributed throughout each ring; (3) objects that are flying entirely within the shell (e.g., GEO orbits) will transit the entire population.

It is the third assumption which is the most questionable, in that one could perform standard GEO stationkeeping maneuvers to ensure that one’s GEO object does not fly past all the other GEO objects. Assumption #3 (above) is more valid for GEO debris collision probability estimations.

However, for the remainder of other RSOs, the above assumptions are considered to be fairly valid. Our goal is to obtain reasonably accurate average collision probability values from which overall observations can be made.

The results are shown in Figure 38 and Figure 39. An obvious result is that even though we concluded that GEO spatial density was higher than that of LEO, the resultant collision probability at GEO is more than an order of magnitude lower than that of LEO. This occurs because GEO objects only have one orbit per day, whereas LEO objects can have more than 15 orbits per day.

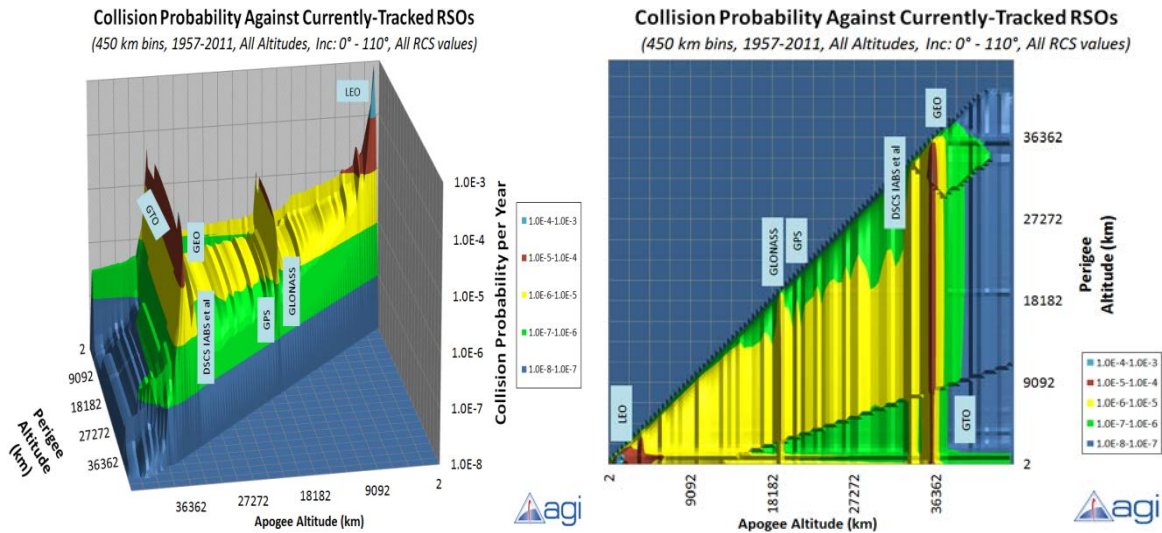


Figure 38. Space Population Perigee-vs-Apogee Distribution (3D)

Figure 39. Space Population Perigee-vs-Apogee Distribution (2D)

ORBIT DISTRIBUTION STATISTICS FACILITATE HYPOTHETICAL CATALOGS

Hypothetical space object catalogs that are significantly larger than our current public-tracked space population allow the space analyst to assess network loading, sensor availability, and model sensor resolution as a function of assigned object sizes. In order of increasing sophistication (and, perhaps, realism), the three principal ways of developing such a catalog are to:

- (1) Examine the existing space population distribution (spanning orbital elements) and simply introduce additional (smaller) debris objects that are consistent with that population;

- (2) Adopt a debris model (such as Master) and use a “splash plate” analysis² or a gridded cell population to create a complete catalog (either starting with the null set or the existing catalog) that is consistent with that model;
- (3) Retain the large space objects currently in the catalog, gather up all known information on all known breakups and explosions (NASA debris digest, etc.), and then run a program such as DEBBIE to model each collision and explosion. Each event will provide several dials/knobs that one could control to provide an overall catalog (after incorporating rapid orbital decay estimation, as DEBBIE does) that matches the desired catalog size.

The statistical distributions shown in this paper easily permit the construction of large hypothetical catalogs consistent with method (1) listed above. To build this catalog, the mean motion (n) distribution (revs/day) is constructed as a function of orbit altitude, across all orbits in the current TLE catalog. Simultaneously, distributions in {"Ecc", "Inc", "RAAN", "w", "BStar"} are collected as a function of the mean motion bins (i.e. dependent distributions as a function of the independent “n” distribution. The use of 1000 bins for all variables appeared to work well.

Then, random draws of percentile (0% - 100%) of the mean motion distribution were accomplished, which in turn identified the dependent variable distributions for the other orbital elements that were also randomly drawn upon for that identified mean motion bin. In doing so, representative random draws of the orbit population distribution are achieved that reflect where space objects actually are instead of arbitrarily selection. Mean anomaly was simply selected based upon random draw from 0 to 360 deg.

We recognize that the distribution of very small particles is not likely to match that of larger ones, but we feel that it probably matches them much better than it does a uniform distribution. Note that BStar may also be randomized outside of the current catalog’s distribution, since small fragments typically will have different BStar terms by nature of being small.

Current limitation on single catalog size is 99,999 objects, since the current NORAD ID is limited to only 5 characters. Such a catalog has been produced and could be made freely available via www.CelesTrak.com. The authors also suggest that by replacing the current integer SSC scheme with an equivalent 5-character hexadecimal representation, catalog sizes containing as many as 1048575 RSOs (FFFFFFh) could be realized.

CONCLUSIONS

The orbital characteristics of our current public space population have been explored. New approaches of computing spatial density and collision probability have been employed. It is felt that the resulting products more accurately portray conditions in space, facilitating a better understanding of relative collision risk as a function of orbit regime, date and orbital characteristics.

FUTURE WORK

Since the space environment is ever-changing, it is proposed that these types of studies be periodically updated to maintain currency. Improvements in space surveillance technology may lead to dramatic evolution of knowledge of our space population, which may require “unscheduled” updates in addition to our regular analysis frequency.

ACKNOWLEDGMENTS

The authors wish to thank AGI’s CSSI technical experts for their insightful comments and review of this paper.

REFERENCES

¹ Finkleman, D. and Oltrogge, D.L., “Twenty-five Years, more or less: Interpretation of the LEO Debris Mitigation 25-Year Post-Mission Lifetime Guideline”, AIAA/AAS Astrodynamics Specialist Conference, Toronto, CA 2010, 14 Aug. 2010.

²Vance, L. and Mense, Allan, “Updated Value Analysis for Orbital Debris Removal: The Business Case”, Raytheon, IAC-10.A6.2.12, 27 Sept. 2010.